Quantum interference of K capture in energetic $Ge^{31+}(1s)$ -Kr collisions

R. Schuch¹, M. Schulz, Y. S. Kozhedub, V. M. Shabaev, I. I. Tupitsyn, G. Plunien, P. H. Mokler, and H. Schmidt-Böcking

¹Physics Department, Stockholm University, Alba Nova, 107 67 Stockholm, Sweden

²Physics Department and LAMOR, Missouri University of Science & Technology, Rolla, Missouri 65409, USA

³Department of Physics, St. Petersburg State University, Universitetskaya 7/9, 199034 St. Petersburg, Russia

⁴NRC "Kurchatov Institute," Academician Kurchatov 1, 123182 Moscow, Russia

⁵Institut für Theoretische Physik, TU Dresden, Mommsenstrasse 13, D-01062 Dresden, Germany

⁶GSI Helmholtzzentrum für Schwerionenforschung, D-64291 Darmstadt, Germany

⁷Department of Physics, Frankfurt University, D-60486 Frankfurt, Germany



(Received 27 November 2019; accepted 24 February 2020; published 2 April 2020)

We have measured characteristic K x rays in coincidence with the scattered particles from collisions of hydrogenlike Ge ions with Kr atoms. The ions were first accelerated to 8.6 MeV/amu, post-stripped to H-like charge state, and decelerated to around 2.5 MeV/amu. From the measurements the probabilities for K-shell to K-shell charge transfer as a function of collision impact parameters were obtained. The probabilities show an onset of oscillations which are interpreted as quantum interference between the K-shell to K-shell electron transfer amplitudes in two spatially separated coupling regions in the incoming and outgoing parts of the collision. The probabilities of K-shell vacancy distribution created by the collision are calculated within a relativistic independent electron model using the coupled-channel approach with atomlike Dirac-Fock-Sturm orbitals. A reasonable agreement between the theoretical results and the experimental data is found.

DOI: 10.1103/PhysRevA.101.042701

I. INTRODUCTION

It has been found in numerous studies that in slow collisions of ions and atoms the atomic states can form moleculelike states, the so-called quasimolecular states [1,2]. This became evident in inner-shell ionization when the collision velocity was smaller than the Bohr velocity of the active electron. Much of the interest in these quasimolecules was triggered by the possibility to create and to study bound states of superheavy quasimolecules [2]. Quasimolecules formed in the short time of energetic heavy ion-atom collisions with $Z_P + Z_T > 1/\alpha$ (Z_P is the ion nuclear charge, Z_T is the target nuclear charge, and α is the fine-structure constant) should allow exploration of quantum electrodynamics of electrons bound in extremely strong fields, far beyond the Schwinger limit [2]. According to the point nuclear Dirac equation the 1s state of a hydrogenlike ion with $Z = 1/\alpha = 137$ dives into the negative continuum. Due to QED effects and the finite nuclear size this limit is pushed up to Z = 173.

The experimental methods for studies of quasimolecular states in this regime range from the detection of characteristic x rays, emitted by the separated atoms [3], and continuum x rays emitted by the quasimolecule [4], to detection of

Published by the American Physical Society under the terms of the Creative Commons Attribution 4.0 International license. Further distribution of this work must maintain attribution to the author(s) and the published article's title, journal citation, and DOI. Funded by Bibsam.

electrons and positrons [5]. For lighter collision systems it was shown that by impact-parameter-dependent measurements of characteristic and continuum x rays, spectroscopic access to the quasimolecules transiently formed in the collision can be reached [4,6]. By analyzing the quasimolecular energies in the limit of small internuclear separation, spectroscopic information could even become available for superheavy atoms which cannot be generated as stationary, but as a temporary system in collisions.

If a K-shell vacancy is brought into the collision by one of the two collision partners of similar nuclear charge, e.g., by using a hydrogenlike ion, then this vacancy can be transferred near resonantly to the other partner [6,7]. At slow collision velocity $v < v_K$, where v_K is the Bohr velocity of the K-shell electron, one has ascribed this to radial coupling between the quasimolecular states $1s\sigma$ and $2p\sigma$ which are formed from the symmetric and antisymmetric superposition of the K-shell states of the heavier and lighter collision partners, respectively. For the coupling to be efficient, the internuclear distance needs to be large enough for the energy difference between the two states to be still small, but small enough for a sufficient overlap between both atomic wave functions of the separated atoms. As a result of this requirement, there are two relatively well localized coupling regions, one in the incoming and one in the outgoing part of the collision. The $1s\sigma$ and $2p\sigma$ radial coupling amplitudes from these coupling regions on the incoming part and outgoing part of the collision trajectory need to be added coherently. This can give rise to a quantum mechanical interference if the phase between the two parts of the amplitudes can be fixed. In the experiment this is done by selecting collision trajectories through a coincidence between

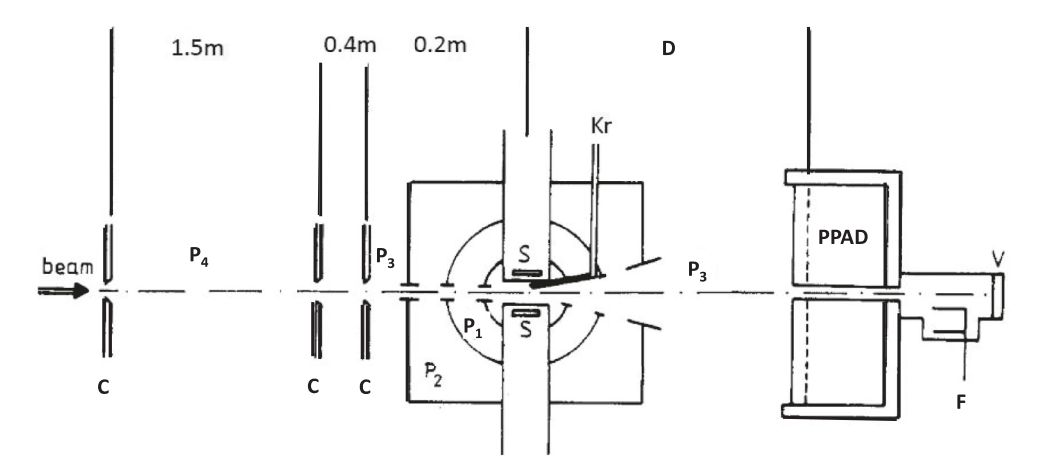


FIG. 1. Schematic experimental setup: C collimators; S: x-ray detectors; P₁: first pumping stage; P₂: second pumping stage; P₃: third pumping stage; P₄: fourth pumping stage; V: viewer; Kr: gas inlet; PPAD: parallel-plate avalanche detector; D: distance PPAD: target (see text); F: Faraday cup.

K-x-ray emission and angle resolved scattered projectiles [8]. From a comparison of the measured Interference structure for varied scattering angles with theoretical calculations, spectroscopic information about the quasimolecular $1s\sigma$ and $2p\sigma$ states can be derived [6]. It is clear that for deriving reliable information on these states and finally about the question of diving of the $1s\sigma$ state into the negative continuum one needs advanced theoretical descriptions on the coupling between the quasimolecular states. Thus it is necessary to test such calculations starting from lighter systems to more and more heavy collisions to keep under control the complex quantum dynamics in such systems, where, e.g., relativistic and QED effects become important.

In this context, a frequently discussed question is the possible loss of coherence between the two parts of interfering amplitudes of *K*-shell transfer on the way in and way out of the collision by simultaneous electron transfer from the neutral target atom to the highly charged ion from higher shells in the collision. That changes the potential and thus the states of the levels [6]. Experiments with medium nuclear charge collision systems, such as Ge and Kr, can give information about this possible problem as here besides the *K*-shell to *K*-shell transfer also a large number of *L*- and *M*-shell electrons are transferred in the selected close collision that creates a large variation in the interaction potential.

Here we present a study of K-shell to K-shell electron transfer probabilities for a medium heavy, low-velocity collision system. For getting the low-velocity H-like Ge ions the accel-decel method [9,10] was applied, where Ge was first accelerated to 8.6 MeV/u to reach high charge states by poststripping, to extract H-like Ge ions. These were then decelerated to an energy around 2.5 MeV/u (we use throughout the paper the abreviation MeV/u for MeV/amu). The collision between these Ge^{31+} ions and Kr atoms can be considered near adiabatic as the ratio between the projectile velocity and the Bohr velocity of the electron to be captured from the Kr K shell is quite a bit smaller than unity (0.3).

The experiment (described in Sec. II) was done a long time ago. At that time a proper theoretical analysis was missing and it remained unpublished. Recently, new interest in such studies arose [11–14] and a theoretical development started [15–17] that can be tested with the present data. A short description of the calculations will be given in Sec. III, followed by the results of the experiments and discussions of the comparison with the theory in Sec. IV.

II. EXPERIMENT

The H-like Ge beam was prepared at the UNILAC of GSI in Darmstadt by the accel-decel method [9,10]. Low-charged Ge ions were accelerated to 8.6 MeV/u and then poststripped to high charge states. These ions were then decelerated by the single resonators of the UNILAC. Hydrogenlike Ge ions could then be energy and charge selected with a yield of about 20% by a 90° dipole magnet and sent to the experiment. The final beam energies were 2.7 MeV/u in the first experiment and 2.45 MeV/u in a later run. A schematic picture of the experimental setup is shown in Fig. 1. The two beam-defining collimators were 1.5 m apart with an additional anti-slitscattering collimator and this limited the angular divergence of the beam to about 2 mrad (which is smaller than even the smallest analyzed scattering angle of 3 and 4 mrad for the two projectile energies). Here a large part of the beam (\approx 90%) was lost due to its large emittance after deceleration.

The ions then hit a thin windowless Kr gas target localized by a three-stage differentially pumped gas cell. In each pumping stage $(P_1 - P_3)$ a drop of about one order of magnitude in pressure was achieved. With a target pressure of 4 mTorr over a length of 10 mm a pressure P_4 in the low 10^{-7} Torr range could be kept in the beam line. With this vacuum the loss of H-like Ge projectiles by capture outside the target gas cell was found negligible.

Two Li-drifted Si x-ray detectors were used for detecting the K x rays of Ge at around 10.5 keV and of Kr at around 13 keV with an efficiency of nearly 100% and a geometrical solid angle Ω of around 4% of 4π . The singles x-ray count rate reached up to 2 kHz in each detector. These were set in coincidence with the scattered particles detected by a parallel plate avalanche detector (PPAD) [18]. The PPAD with a 16-ring anode was mounted at D=1.27 m (2.7 MeV) and

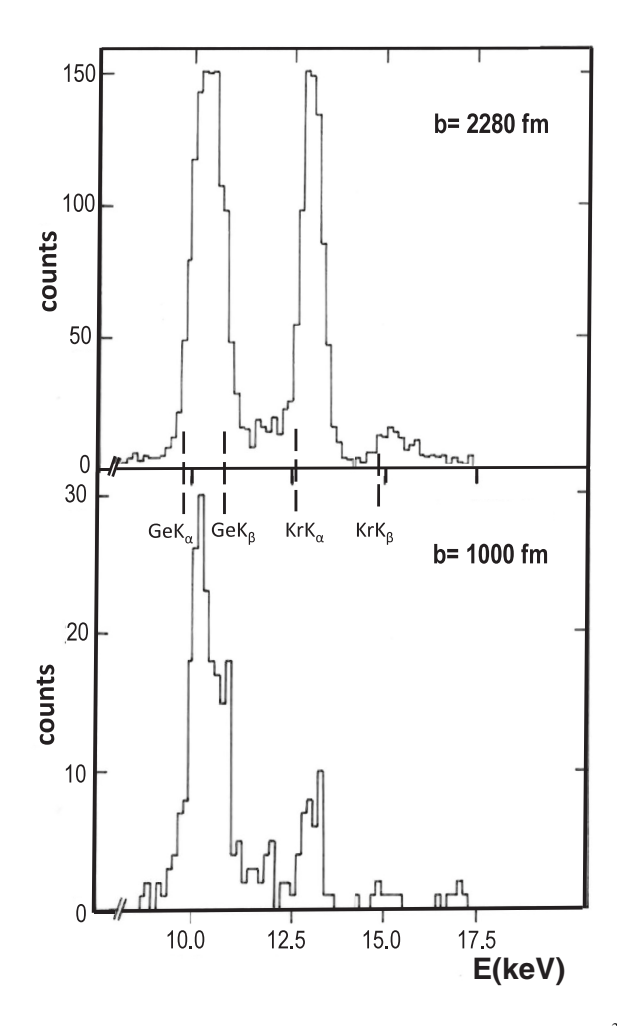


FIG. 2. True coincident K x-ray spectra for 2.45 MeV/u Ge³¹⁺ on Kr at two different impact parameters b. Vertical dashed lines indicate the positions of the neutral atom energies of projectile Ge K_{α} , Ge K_{β} , and target Kr K_{α} , Kr K_{β} .

 $D=1.71\,\mathrm{m}$ (2.45 MeV) from the target covering a scattering angle range from 0.1° to 0.7° and 0.2° to 2° , respectively. All parameters of the experiment were stored in event mode. In order to convert the coincident count rates to probabilities, they were normalized to the detected scattered projectile count rates. The high x-ray singles count rates could generate considerable pile-up events. These were suppressed by electronically setting a pile-up rejection system based on the different rise times of an x ray and a pile-up pulse.

For getting the impact-parameter-dependent K-shell capture probabilities, the true coincident events for each scattering angle interval (ring of the PPAD anode) had to be extracted. Two such true coincident spectra from $2.45 \,\mathrm{MeV/u}\,\mathrm{Ge^{31+}} + \mathrm{Kr}$ collisions are shown in Fig. 2 for impact parameters of $b = 2280 \,\mathrm{fm}$ and $b = 1000 \,\mathrm{fm}$. These spectra already demonstrate the effect of a constructive and destructive interference in quasiresonant K-shell to K-shell charge transfer. The $\mathrm{Kr}\,K$ lines at about 13 keV are as intense as the $\mathrm{Ge}\,K$ lines at about 10.5 keV at the larger impact parameter of 2280 fm. This is very different from the situation at smaller b of 1000 fm where the Kr line is much weaker than the Ge line. Without interference one would expect the

transfer probability to remain roughly constant or even increase with decreasing impact parameter. Instead, the transfer of Kr K-shell electrons is obviously at smaller b strongly reduced by a destructive interference of the amplitudes.

The true coincident Ge and Kr K line intensities N_{Ge} and $N_{\rm Kr}$ have to be divided by the number of (slit-scatteringcorrected) detected particles N_p , the corresponding fluorescence yield $\omega_{\text{Ge/Kr}}$, and solid angle Ω to obtain the K-shell vacancy probabilities P_{Ge} and P_{Kr} , respectively. An advantage of heavier collision systems is that for Z > 30 radiative decay becomes dominant over Auger decay. Therefore, the use of neutral-atom fluorescence yield values ($\omega_{Kr} = 0.66$ and $\omega_{\rm Ge} = 0.554$) does not cause too big an uncertainty. There remains a possible ω dependence on the populations of L and M shells and on their possible dependencies on impact parameter. One can argue that the impact parameter range studied here selects close collisions, certainly for L- and M-shell ionization and capture, so that charge equilibration occurs concerning L- and M-shell population that determines ω [19]. One can assume that these populations of the L and M shell do not change in the narrow impact parameter range that we consider. Some evidence for these assumptions can be seen in Fig. 2 in the shifts of the projectile and target K_{α} and K_{β} lines, respectively, from the neutral atom values. The Ge and Kr lines are both shifted by roughly the same amount, and the shift also does not vary visibly with the impact parameter. This finding is also strongly supported by an earlier measurement that was done for the lighter collision system S-Ar [20]. There, one is more sensitive to a possible dependence of the fluorescence yields on b and no dependence in a similar b range was found.

Correcting the measured K x-ray intensities for the fluorescence yield and the detector solid angle, the K-vacancy probabilities are given by $P_{\text{Ge/Kr}} = N_{\text{Ge/Kr}}/(\omega_{\text{Ge/Kr}}\Omega N_p)$. On the other hand, as we use H-like ions, one K vacancy is initially present in the projectile. If we assume that this vacancy is either transferred to the Kr K shell or remains in the Ge K shell and that no additional K vacancies are produced in the collision then $P_{\text{Ge}} + P_{\text{Kr}} = 1$. However, it is well known that, especially at small impact parameters, K-vacancy production through rotational coupling between the $2p\pi$ and $2p\sigma$ quasimolecular states can occur with nonnegligible probability. The total K-vacancy probability is then given by $P_{\text{Ge}} + P_{\text{Kr}} = 1 + P_{\text{rot}}$, where P_{rot} is the probability for producing an additional K vacancy in the collision (explained further below). Using $P_{Ge} + P_{Kr} = (N_{Kr} +$ $\omega_{\rm Kr}/\omega_{\rm Ge}N_{\rm Ge})/(\omega_{\rm Kr}\Omega N_p)$ the K vacancy probability in Kr is then modified to read $P_{Kr} = N_{Kr}(1 + P_{rot})/(N_{Kr} + aN_{Ge})$, with $a = \omega_{\rm Kr}/\omega_{\rm Ge}$.

If we, to start with, assume $P_{\rm rot} \ll 1$ then $P_{\rm Kr} = N_{\rm Kr}/(N_{\rm Kr} + aN_{\rm Ge})$. The ratio of fluorescence yields of Ge and Kr should be very close to the neutral atom value, much closer than the individual ω values. Using Larkins law [21] and an estimate of four electrons in the L shell of Kr as well as Ge we get for $a = \omega_{\rm Kr}/\omega_{\rm Ge}$ a value of $a \simeq 1.1$ instead of 1.19 using the neutral atoms fluorescence yields.

The scattering angles were converted into impact parameters by using a screened Bohr potential. The calculated impact parameters showed deviations from those calculated for an unscreened Rutherford trajectory of less than 2% for the smallest

scattering angles and became smaller for larger angles. The error bars shown in the figures in the next sections are only the statistical errors. Furthermore, the determination of all total probabilities is affected by a systematic error, mainly resulting from uncertainties in determining the correct fluorescence yield ratio being used. Our estimate for the average (impact-parameter-dependent) systematic error is 15%.

III. THEORY

In the following, we briefly present the formalism used; for a complete description see Refs. [15–17]. Using the semiclassical approximation, where the atomic nuclei move along classical trajectories and are considered as sources of a time-dependent external potential, we have to solve the time-dependent many-particle Dirac equation for electrons involved in the process. We employ the method, which is based on an independent particle model, where the many-electron Hamiltonian H is approximated by a sum of effective single-electron Hamiltonians, $H^{\text{eff}} = \sum_j h_{\rm eff}^{\rm eff}$, reducing the electronic many-particle problem to a set of single-particle Dirac equations for all (N) electrons of the colliding system:

$$i\frac{\partial \psi_j(\mathbf{r},t)}{\partial t} = h_j^{\text{eff}}(\mathbf{r},t)\psi_j(\mathbf{r},t) \text{ with } j=1,\ldots,N,$$

where the one-electron wave functions $\psi_j(\mathbf{r}, t)$ are subject to the initial conditions $\psi_i^0(\mathbf{r}, t)$:

$$\lim_{t \to -\infty} (\psi_i(\mathbf{r}, t) - \psi_i^0(\mathbf{r}, t)) = 0 \text{ with } j = 1, \dots, N.$$

As the effective single-electron Hamiltonian h^{eff} we use the two-center Dirac-Kohn-Sham Hamiltonian:

$$h^{\text{eff}} = c(\boldsymbol{\alpha} \cdot \boldsymbol{p}) + \beta c^2 + V_{\text{nucl}}^A(\boldsymbol{r}_A) + V_{\text{nucl}}^B(\boldsymbol{r}_B) + V_C[\rho] + V_{xc}[\rho],$$

where c is the speed of light and α , β are the Dirac matrices. Here $V^{\alpha}_{\mathrm{nucl}}(\mathbf{r}_{\alpha})$ and $V_{C}[\rho] = \int d^{3}\mathbf{r}' \frac{\rho(\mathbf{r}')}{|\mathbf{r}-\mathbf{r}'|}$ are the electron-nucleus and the electron-electron Coulomb interaction potentials, respectively; index $\alpha = A$, B indicates the centers; $\mathbf{r}_{\alpha} = \mathbf{r} - \mathbf{R}_{\alpha}$, \mathbf{R}_{α} is the center (nuclear) coordinate; and $\rho(\mathbf{r})$ is the electron density of the system. The exchange-correlation potential $V_{xc}[\rho]$ is taken in the Perdew-Zunger parametrization [22]. V_{C} and V_{xc} together provide the electron screening potential.

Solving the effective single-particle equations is based on the coupled-channel approach with atomiclike Dirac-Sturm-Fock orbitals, localized at the ions (atoms) [15]. Within this approach, the one-electron wave functions are represented as

$$\psi_j(\mathbf{r},t) = \sum_{a=A.B} \sum_a C^j_{\alpha,a}(t) \chi_{\alpha,a}(\mathbf{r}_\alpha,t),$$

where the index a enumerates basis functions at the given center, and $\chi_{\alpha,a}(\mathbf{r}_{\alpha},t)$ is the center-field bispinor centered at the point α . The insertion of the expansion into the time-dependent Dirac equation leads to the coupled-channel

equations for the coefficients $C_{\alpha,a}^{j}(t)$,

$$\begin{split} i \sum_{\beta,b} \langle X_{\beta,b} | X_{\alpha,a} \rangle \frac{dC_{\beta,b}^{j}(t)}{dt} \\ &= \sum_{\beta,b} \langle X_{\alpha,a} | \left(h_{j}^{\text{eff}} - i \frac{\partial}{\partial t} \right) | X_{\beta,b} \rangle C_{\beta,b}^{j}(t), \end{split}$$

where the indices α , a and β , b enumerate the basis functions of both centers. The direct evolution (exponential) operator method [15] is employed in order to obtain the expansion coefficients. The many-particle probabilities are calculated in terms of the single-particle amplitudes employing the formalism of inclusive probabilities [23,24], which allows one to describe the many-electron collision dynamics. By solving the general eigenproblem for the matrix of the $(h_j^{\rm eff} - i \frac{\partial}{\partial t})$ operator within the used basis set we obtain time-dependent quasimolecular states and study their populations during the collisions.

The evaluation of P_{Kr} and P_{Ge} requires an independent consideration of the K-shell populations of the target (Kr) and projectile (Ge). Thus P_{Kr} (P_{Ge}) values were calculated as sums of probabilities to find exactly one vacancy plus the double probability to find exactly two vacancies in the K shell of Kr (Ge), while the K-shell population of Ge (Kr) was arbitrary. A coupled-channel basis set, consisting of atomic shells 1s-8s, 2p-9p, 3d-10d, 4f-11f, and 1s-7s, 2p-7p, 3d-7d, 4f-7f (in standard nonrelativistic notation) of the Dirac-Fock-Sturm orbitals on the target and projectile, respectively, was used. Based on the calculations combined with a variation of the basis set we estimate the accuracy of the obtained values to be on the 5% level. The calculations were carried out in the laboratory coordinate system, where the target atom (Kr) initially is at rest. In order to study the role of relativistic effects, we also performed the calculation in the nonrelativistic limit using the same computing routine, but multiplying the standard value of the speed of light by a factor of 1000. As a result we conclude that relativistic effects do not change the shape of P(b) significantly, but only shift the nonrelativistic P(b) to smaller impact parameters in the region around 100 fm.

IV. RESULTS AND DISCUSSION

In Figs. 3 and 4 the $P_{Kr}(b)$ and $P_{Ge}(b)$ are plotted for collision energies of 2.7 and 2.45 MeV/u, respectively. The calculated values are shown by dashed and solid lines. One can clearly see in the data the onset of oscillations as a function of b in the two data sets. The experiment covered only a small range at small b relative to the large b range where according to the theory K-K-shell transfer occurs with considerable probability. $P_{Kr}(b)$ extends with a considerable magnitude to very large b, more than three times the mean K-shell radius of around 1500 fm. For two reasons the range at small b is, however, the most interesting part of b where the theory is to be tested: In this b range, corresponding to close collisions, the strongest binding occurs in the $1s\sigma$ molecular orbital. Second, in this b range couplings to other molecular orbitals also operate, especially the $2p\pi$ - $2p\sigma$ rotational coupling [25] and possibly direct ionization [26] from the $1s\sigma$

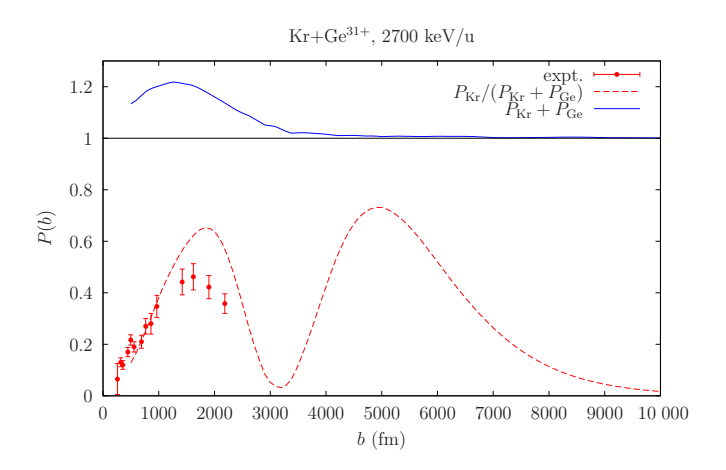


FIG. 3. The plot of P(b) shows the target Kr K-shell probability $P_{\rm Kr}(b)$ normalized to the total K-shell probability $P_{\rm Kr} + P_{\rm Ge}$ (lower part, dashed red line) and the total K-shell probability $P_{\rm Kr} + P_{\rm Ge}$ (upper part, solid blue line) as functions of impact parameter b for collision energy of 2.7 MeV/u.

and $2p\sigma$ molecular orbitals. These channels could change the magnitude of P(b) and shift the phase in the interference term. The additional vacancy production by $2p\pi$ - $2p\sigma$ rotational coupling $P_{\text{rot}}(b)$ is seen in the upper curves of Figs. 3 and 4 in the increase of the sum of K-vacancy production above unity at b around 1000 fm. Experimentally the contribution from $P_{\text{rot}}(b)$ can be estimated from the measurements of Ref. [9], where the K vacancy production in the Kr-Kr collision at only slightly higher collision energy of 2.8 MeV/u and charge states of up to 33+ was measured and a maximum probability of around 0.25 was found. This is in excellent agreement with the results of our calculations. The contribution by this additional K-vacancy production is taken into account in the comparison of the Ge-Kr data with the theory.

The deviation of the 2.7 MeV data from the calculation in absolute magnitude could have the following reason. The magnitude of the structures depends on the existence of a

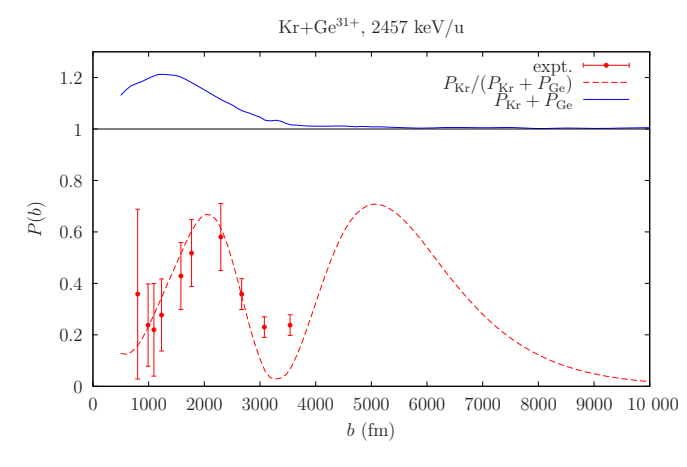


FIG. 4. The plot of P(b) shows the target Kr K-shell probability $P_{\rm Kr}(b)$ normalized to the total K-shell probability $P_{\rm Kr}+P_{\rm Ge}$ (lower part, dashed red line) and the total K-shell probability $P_{\rm Kr}+P_{\rm Ge}$ (upper part, solid blue line) as functions of impact parameter b for collision energy of 2.45 MeV/u.

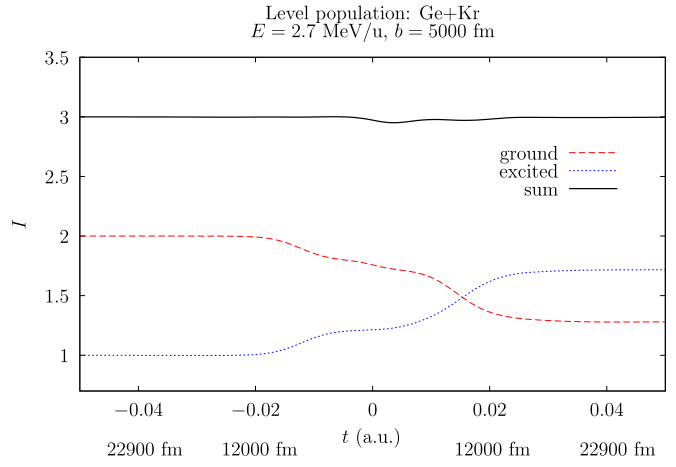


FIG. 5. Population I of the ground (dashed red line) and first excited (dotted blue line) quasimolecular energy levels and the sum of them (solid black line) depending on collision time and internuclear distance for the impact parameter b = 5000 fm in $2.7 \,\mathrm{MeV/u}$ Ge³¹⁺-Kr collisions.

projectile *K*-shell vacancy in the incoming part of the close collisions. Therefore, a crucial point for the normalization of the experimental data is to ensure that the majority of the initial *K* vacancies brought into the collision via hydrogenlike projectiles survive the passage to the close collision. There could, however, be electron capture from the residual gas before the ion reaches the relevant target region. The impact of this effect on the *K-K* transfer probabilities involves a delicate balance between the target pressure and the vacuum in the beamline and may contribute, apart from the fluorescence yield ratio, mostly to the systematic error in height that was estimated to be 20%.

In the following run we were able to decrease the collision energy a bit more to 2.45 MeV/u. Furthermore, the projectile detector was placed at a larger distance from the target. As a result, we were able to cover a b range at somewhat larger values. With that we can identify the second minimum in the $P_{\rm Kr}(b)$ oscillation. Also the absolute magnitude of $P_{\rm Kr}(b)$ is now a bit higher which indicates a smaller systematic error in the normalization of the data as compared to the 2.7 MeV/u measurement. Both the magnitude of the probability and the maximum and minimum of the oscillation, i.e., the phase in the interference term, are in very good agreement with the calculation. This also means that the data do not provide any indications for a significant loss of coherence (which would wash out the interference pattern) due to capture in the outer shells (see the Introduction).

In Fig. 5 the populations I of the two lowest quasimolecular levels, ground 1σ and excited $1\sigma^*$ (corresponding to the $1s\sigma$ and $2p\sigma$ molecular orbitals, the dashed red and dotted blue curves, respectively), during collision at the collision energy $E=2.7\,\mathrm{MeV/u}$ and impact parameter $b=5000\,\mathrm{fm}$ are presented. Due to the initial K vacancy in Ge the total value of I starts with a value of exactly 3. One can see that the electron and vacancy densities are distributed between the levels under consideration during the collision. Transitions between the levels occur at two time intervals: $\Delta t_1 \sim (-0.02, -0.01)$ and $\Delta t_2 \sim (0.01, 0.02)$ around t_1 and t_2 on incoming and

outgoing parts of the trajectory, respectively. This is due to the strongest radial couplings there. In the sum of the populations I (Fig. 5) one sees also some excitation (but rather small) to higher energy levels at the zero time region due to rotational coupling.

The final values of level population in Kr and Ge K shells and its oscillatory behavior (see Figs. 3 and 4) arise from a coherent superposition of two transition amplitudes at the time intervals Δt_1 and Δt_2 . This view is analog to the atomic clock principle of Ramsey's "separated oscillating field method" [27]. In Ramsey's pioneering experiment fast moving atoms pass through two coherent resonators and they can be excited in either resonator 1 or 2. Since the experimenter cannot decide in which resonator the excitation took place both excitation amplitudes have to be added coherently which gives rise to oscillations. In the ion-atom collision processes of hydrogenlike Ge³¹⁺ projectiles on Kr atoms that we report, one can use the fast classical motion of the ions as a very fast clock. This is done by measuring the K x rays in coincidence with scattered projectiles to select, by the scattering angle, a well defined impact parameter. From the interference structure and trajectory parameters one could obtain electronic dynamics with better than attosecond time resolution for the case under consideration.

V. CONCLUSION

We determined the probabilities for *K*-shell to *K*-shell charge transfer as a function of impact parameter for decelerated hydrogenlike Ge ions colliding with Kr atoms. From the observed onset of oscillations we conclude the appearance of quantum interferences between the *K*-shell to *K*-shell electron transfer amplitudes in two spatially separated coupling regions in the incoming and outgoing parts of the collision. The probabilities of *K*-shell vacancy distribution

created by the collision are calculated within a relativistic independent electron model using the coupled-channel approach with atomiclike Dirac-Fock-Sturm orbitals. A quite good agreement between the theoretical results and the experimental data is found. The appearance of interference in the 1s to 1s electron transfer probability as a function of impact parameter demonstrates that the phase coherence is not lost even in these slow heavy collisions with this very large charge asymmetry on the entrance channel of the collision. Given this charge asymmetry of Ge³¹⁺ and neutral Kr atoms and given the selection of close collisions it can be expected that a large number of target L and M shell electrons will be transferred in the collisions. The calculations verify the phase and amplitude of the P(b) very well, in spite of the selected rather small impact parameters where rotational coupling contributes strongly. It is discussed how one can use the interference structure and trajectory parameters for a very fast clock in visualizing electronic dynamics with better than attosecond time resolution. These results are very encouraging for the proposals to proceed to heavier collision systems with the ultimate goal to create and to study bound states of superheavy quasimolecules and to search for diving of these states into the negative energy continuum.

ACKNOWLEDGMENTS

This work was supported by RFBR (Grants No. 18-32-20063 and No. 18-03-01220) and by SPbSU-DFG (Grants No. 11.65.41.2017 and No. STO 346/5-1) and by using computational resources provided by the Resource Center "Computer Center of SPbSU". Y.S.K. acknowledges support from SPbSU (COLLAB 2019: No. 41160833), and V.M.S. the support by the Foundation for the Advancement of Theoretical Physics and Mathematics "BASIS." M.S. was supported by a grant from NSF (Grant No. PHY-1703109).

- W. Lichten, Phys. Rev. 131, 229 (1963); 139, A27 (1965); for more recent publications see, for example, L. Ph. H. Schmidt, M. Schöffler, C. Goihl, T. Jahnke, H. Schmidt-Böcking, and R. Dörner, Phys. Rev. A 94, 052701 (2016).
- [2] G. Soff, B. Müller, and W. Greiner, Phys. Rev. Lett. 40, 540 (1978).
- [3] P. H. Mokler, D. Liesen, in *Progress in Atomic Spectroscopy, Part C*, edited by H. F. Beyer, and H. Kleinpoppen (Plenum Publishing, New York, 1984), p. 321.
- [4] R. Schuch, M. Meron, B. M. Johnson, K. W. Jones, R. Hoffmann, H. Schmidt-Böcking, and I. Tserruya, Phys. Rev. A 37, 3313 (1988).
- [5] T. Cowan, H. Backe, K. Bethge, H. Bokemeyer, H. Folger, J. S. Greenberg, K. Sakaguchi, D. Schwalm, J. Schweppe, K. E. Stiebing, and P. Vincent, Phys. Rev. Lett. 56, 444 (1986).
- [6] R. Schuch, H. Ingwersen, E. Justiniano, H. Schmidt-Böcking, M. Schulz, and F. Ziegler, J. Phys. B: At. Mol. Phys. 17, 2319 (1984).
- [7] F. P. Ziemba and A. Russek, Phys. Rev. 115, 922 (1959); F. P. Ziemba and E. Everhart, Phys. Rev. Lett. 2, 299 (1959); F. P. Ziemba, G. J. Lockwood, G. H. Morgan, and E. Everhart, Phys. Rev. 118, 1552 (1960).

- [8] R. Schuch, G. Nolte, H. Schmidt-Böcking, and W. Lichtenberg, Phys. Rev. Lett. 43, 1104 (1979).
- [9] R. Schuch, E. Justiniano, R. Hoffmann, W. Schadt, H. Schmidt-Böcking, P. H. Mokler, F. Bosch, W. A. Schönfeldt, and Z. Stachura, J. Phys. B: At. Mol. Phys. 16, 2029 (1983).
- [10] P. H. Mokler, D. H. H. Hoffmann, W. A. Schönfeldt, D. Maor, Z. Stachura, and A. Warczak, J. Phys. B: At. Mol. Phys. 17, 4499 (1984).
- [11] P. Verma, P. H. Mokler, A. Bräuning-Demian, H. Bräuning, M. Schöffler, F. Bosch, Th. Stöhlker, S. Hagmann, D. Liesen, C. Kozhuharov, S. Toleikis, D. Banas, S. Tashenov, A. Orsic-Muthig, U. Spillmann, D. Sierpowski, Z. Stachura, and M. A. Wahab, Nucl. Instrum. Methods Phys. Res. Sect. B 245, 56 (2006).
- [12] S. Hagmann, Th. Stöhlker, Ch. Kozhuharov, V. Shabaev, I. Tupitsyn, Y. Kozhedub, H. Rothard, U. Spillmann, R. Reuschl, S. Trotsenko, F. Bosch, D. Liesen, D. Winters, J. Ullrich, R. Dörner, R. Moshammer, P.-M. Hillenbrand, D. Jakubassa-Amundsen, A. Voitkiv, and A. Surzhykov et al., in Application of Accelerators in Research and Industry—2010, Fort Worth, TX, Proceedings of the 21st International Conference, AIP Conf. Proc. No. 1336, edited by F. D. McDaniel and B. L. Doyle (AIP, New York, 2011), p. 115.

- [13] A. Gumberidze, C. Kozhuharov, R. T. Zhang, S. Trotsenko, Y. S. Kozhedub, R. D. DuBois, H. F. Beyer, K.-H. Blumenhagen, C. Brandau, A. Bräuning-Demian, W. Chen, O. Forstner, B. Gao, T. Gassner, R. E. Grisenti, S. Hagmann, P.-M. Hillenbrand, P. Indelicato, A. Kumar, and M. Lestinsky et al., Nucl. Instrum. Methods Phys. Res. Sect. B 408, 27 (2017).
- [14] C. Shao, D. Yu, X. Cai, X. Chen, K. Ma, J. Evslin, Y. Xue, W. Wang, Y. S. Kozhedub, R. Lu, Z. Song, M. Zhang, J. Liu, B. Yang, Y. Guo, J. Zhang, F. Ruan, Y. Wu, Y. Zhang, and C. Dong *et al.*, Phys. Rev. A **96**, 012708 (2017).
- [15] I. I. Tupitsyn, Y. S. Kozhedub, V. M. Shabaev, G. B. Deyneka, S. Hagmann, C. Kozhuharov, G. Plunien, and Th. Stöhlker, Phys. Rev. A 82, 042701 (2010).
- [16] Y. S. Kozhedub, I. I. Tupitsyn, V. M. Shabaev, S. Hagmann, G. Plunien, and T. Stöhlker, Phys. Scr. T156, 014053 (2013).
- [17] Y. S. Kozhedub, V. M. Shabaev, I. I. Tupitsyn, A. Gumberidze, S. Hagmann, G. Plunien, and Th. Stöhlker, Phys. Rev. A 90, 042709 (2014).

- [18] G. Gaukler, H. Schmidt-Böcking, R. Schuch, R. Schule, H. J. Specht, and I. Tserruya, Nucl. Instrum. Methods 141, 115 (1977).
- [19] D. Maor, B. Rosner, M. Meron, H. Schmidt-Böcking, and R. Schuch, J. Phys. B: At. Mol. Phys. 14, 693 (1981).
- [20] C. L. Cocke, H. Schmidt-Böcking, and R. Schuch, J. Phys. B: At. Mol. Phys. **15**, 651 (1982).
- [21] F. P. Larkins, J. Phys. B: At. Mol. Phys. 4, L29 (1971).
- [22] J. P. Perdew and A. Zunger, Phys. Rev. B 23, 5048 (1981).
- [23] H. J. Lüdde and R. M. Dreizler, J. Phys. B: At. Mol. Phys. 18, 107 (1985).
- [24] P. Kürpick and H. J. Lüdde, Comput. Phys. Commun. 75, 127 (1993).
- [25] K. Taulbjerg, J. Briggs, and J. Vaaben, J. Phys. B: At. Mol. Phys. 9, 1351 (1976).
- [26] G. N. Ogurtsov, V. M. Mikoushkin, S. Yu. Ovchinnikov, and J. H. Macek, J. Phys. B: At. Mol. Phys. 47, 175201 (2014).
- [27] N. F. Ramsey, Phys. Rev. 78, 695 (1950); Rev. Mod. Phys. 62, 541 (1990).